Eur Biophys J (1988) 16: 287–297

European Biophysics Journal

Molecular dynamics simulations of ribonuclease T1

Effect of solvent on the interaction with 2′GMP

A. D. MacKerell Jr. [1,*,**], **R. Rigler** [1], **L. Nilsson** [1], **U. Heinemann** [2], **and W. Saenger** [2]

[1] Department of Medical Biophysics, Karolinska Institutet, S-104 01 Stockholm, Sweden
[2] Institute for Crystallography, Free University Berlin, Takustrasse 6, D-1000 Berlin, Germany

Received March 10, 1988/Accepted in revised form August 3, 1988

Abstract. Molecular dynamics simulations in vacuum and with a water sphere around the active site were performed on the 2′GMP-RNase T1 complex. The presence of water led to the maintenance of the 2′-GMP-RNase T1 interactions as compared to the X-ray structure, including the hydrogen bonds implicated in the enzyme-inhibitor recognition process. The sidechain of *His*92 in the molecular dynamics water simulation, however, hydrogen bonds directly to the phosphate of 2′GMP in contrast to the X-ray structure but in support of the role of that residue in the enzyme's catalytic mechanism. Fluctuations of active-site residues are not strongly influenced by water, possibly owing to the exclusion of water by the bound 2′GMP, which did show an increase in mobility. Analysis of the 2′GMP-RNase T1 interactions versus time reveal an equilibrium fluctuation in the presence of water, leading to a less favorable 2′GMP-RNase T1 interaction energy, suggesting a possible relationship between picosecond fluctuations and inhibitor dissociation occurring in the millisecond time domain.

Key words: Ribonuclease T1, protein dynamics, molecular dynamics, protein-nucleic acid interaction

Introduction

Nucleic acid-protein interactions comprise an aspect of protein function which is important in various physiological roles as well as being an area applicable to the development of various pharmaceutical agents and research tools. Such interactions can be grouped into those involving double-stranded forms of nucleic acids and those involving single-stranded species. The first category is represented by a variety of endonucleases and DNA binding proteins with the most well studied system perhaps being the endonuclease *Eco*R1 for which the crystal structure of the substrate-enzyme complex has been determined (Frederick et al. 1984; McClarin et al. 1986). Ribonuclease A is probably the most well studied enzyme in the second category on which a variety of experimental work (Richards and Wyckhoff 1971; Blackburn and Moore 1982) and theoretical studies (Brünger et al. 1985; Brooks et al. 1986) have been performed. Another enzyme in the second category which has a higher specificity of interaction than RNase A and has also been subjected to extensive study is Ribonuclease T1 (Uchida and Egami 1971; Egami et al. 1980; Takahashi and Moore 1982).

Ribonuclease T1 recognizes guanylic acid residues in single-stranded RNA and catalyzes the cleavage of 3′5′ phosphodiester linkages yielding terminal 3′-guanylic acids (Uchida and Egami 1971; Egami et al. 1980; Takahashi and Moore 1982). Crystallographic studies have been performed on the 2′GMP (Heinemann and Saenger 1982; Sugio et al. 1985a; Arni et al. 1988), the 3′GMP (Sugio et al. 1985b) and, recently, the guanylyl 2′-5′-guanosine (Koepke et al., manuscript in preparation) enzyme forms. These studies reveal a similar guanine-protein interaction pattern for both inhibitors where the base is sandwiched between two tyrosine residues (42 and 45) and a series of hydrogen bonds are formed with residues 43 to 46 and 98, which appear to be responsible for the specificity. Differences, however, do occur in the phosphate-protein interactions, with the change in the position of the phosphate in 2′GMP versus 3′GMP leading to different hydrogen bonding patterns with residues involved in catalysis (Nishikawa et al. 1987). Beyond the

* To whom offprint requests should be sent
** Present address: Department of Chemistry, Harvard University, 12 Oxford Street, Cambridge, Massachusetts 02138, USA

Abbreviations: RNase T1: Ribonuclease T1 (EC.3.1.27.3); 2′GMP: Guanosine-2′-monophosphate; SBS: Stochastic Boundary Simulation: VS: Vacuum Simulation; MD: Molecular Dynamics

direct nucleic acid-protein interactions time-resolved fluorescence depolarization experiments have indicated the presence of conformational and dynamical changes in the protein upon binding of 2′GMP and 3′GMP (MacKerell et al. 1987a, b). To further understand the nature of the interactions between ribonuclease T1 and the above inhibitors, allowing for the interpretation of experimental results and the potential of predictions on altering the specificity of interaction and function of the enzyme, the theoretical technique of molecular dynamics holds great potential.

Molecular dynamics simulations (Karplus and McCammon 1981; McCammon 1984; Warshel 1984) have greatly increased the understanding of the molecular basis of the motions of macromolecules. Applications of the technique are now quite broad (McCammon and Harvey 1987) and correlation with experimental work is often obtained. Variations of the MD approach, including umbrella sampling techniques, brownian dynamics and the thermodynamic perturbation approach, are in rapid development further expanding the use of the technique. Limitations, however, are many with one of the most significant being the computational time required. To deal with this problem a variety of assumptions are made, often including the neglection of the explicit representation of solvent in the simulations. This assumption has been tested with BPTI (van Gunsteren and Karplus 1982a; Swaminathan et al. 1982; van Gunsteren and Berendsen 1984) and with parvalbumin (Ahlström et al. 1987), indicating the alteration of surface side-chain motions although agreement of the effect on motions within the protein interior is lacking.

In the present study the influence of solvent on the interaction between 2′GMP and ribonuclease T1 is analyzed using MD simulations in the presence and absence of solvent. The analysis is restricted to the macromolecular behavior and interactions; work is in progress on the solvent dynamics and structure and will be presented elsewhere. Advantages of using this system, along with the high specificity of interaction and the various experimental studies listed above, are the enzyme's low molecular weight, 11,085 daltons, and its relative structural simplicity, being comprised of only a single α-helix, two β-pleated sheets and several loop regions (Arni et al. 1988). To save computer time and allow for a relatively long trajectory stochastic boundary conditions were employed allowing the maintenance of water in the active-site region (Adelman 1980; Berkowitz and McCammon 1982; Brooks and Karplus 1983; Brünger et al. 1984; Brooks et al. 1985; Brünger et al. 1985). Results from the two simulations are compared with the nucleic acid-protein interactions observed in the 1.9 Å resolution X-ray coordinates for the 2′GMP-RNase T1 complex (Arni et al. 1988).

Methods

Molecular dynamics simulations were performed on NORD-500 and CRAY-1 computers using the program CHARMM (Brooks et al. 1983). Parameters were those currently supported by CHARMM (Brooks et al. 1983), except in the case of 2′GMP. Since there is no explicit hydrogen bonding potential in the protein empirical energy function the charge on each 2′GMP atom was increased by 20% (Reiher III 1985). A net charge of -1.05 was used for the 2′GMP molecule.

The same strategy was used in the present study as in previous MD studies on the free-enzyme form of RNase T1 (MacKerell et al. 1988) allowing some of the methodological details to be omitted. The 1.9 Å refined coordinates for the 2′GMP-RNase T1 complex (Arni et al. 1988) were used as the starting point for the MD simulations. The histidines (27, 40 and 92) where set to doubly protonated $+1$ charge states to correspond with the X-ray data at pH 5 (Heinemann and Saenger 1982; Arni et al. 1988) and experimental data indicating those residues to be protonated at that pH (Rüterjans and Pongs 1971; Arata et al. 1979).

The water representation used was the TIP3P model (Jorgensen et al. 1983). In the Stochastic Boundary Simulation (SBS) all of the 91 waters in the asymmetric unit identified by the X-ray crystallography were included along with an 18 Å radius sphere of water centered around *Tyr*42 OH. The sphere was positioned using information from previous simulations and preparation of the water followed the same procedure as previously published. (MacKerell et al. 1988). Water density within the 18 Å sphere was maintained by the use of a 20.5 Å constraining potential (Warshel 1979; Warshel and Russel 1984; Brooks et al. 1985).

Partitioning of the residues in the SBS was done into a full MD region within the 18 Å sphere and a Langevin region outside of the sphere. A friction coefficient of 50 ps^{-1} was used for the Langevin dynamics. Following the preparation of the system as previously stated (MacKerell et al. 1988) the entire system was energy minimized for 200 Steepest-Descent Steps with harmonic constraints on the protein atoms which were gradually decreased every 40 steps. SHAKE (Ryckaert et al. 1977; van Gunsteren and Karplus 1982b) was used to constrain all covalent bonds involving hydrogen atoms and an integration time-step of 0.02 ps was used. The non-bonded list was updated every 10 steps using a cutoff of 8.0 Å and both the electrostatic and van der Waals potentials were shifted to obtain a smooth transition to zero at 7.5 Å. Initiation of the MD run was performed by instantaneously assigning all atoms with random velocities yielding an overall kinetic energy of 314 K. The system was initially al-

lowed to equilibrate for 20 ps using a temperature window of ± 10 K with checking every 0.1 ps and rescaling when necessary followed by application of a ± 2 K temperature window with checking every 0.1 ps which was maintained for the remainder of the trajectory.

In the vacuum simulation (VS) the X-ray structure was first energy minimized via 200 Adopted-Basis Newton Raphson (Brooks et al. 1983) steps followed by an instantaneous assignment of random velocities to all atoms corresponding to a temperature of 310 K. During the equilibration period of 20 ps a temperature window of ± 10 K with checking every 0.1 ps and rescaling when necessary was applied which was then changed to ± 2 K for the remainder of the simulation. The electrostatic potential was shifted and the van der Waals potential switched (Brooks et al. 1983) to obtain gradual cutoffs which went to zero at 7.5 Å.

Coordinate sets selected every 0.1 ps were used in the analysis of the trajectories. Time-averaged coordinates from the two simulations along with X-ray coordinates were energy minimized for 120 steps with gradually decreasing harmonic constraints on all atoms prior to analysis. RMS differences, Δr, following least-squares fit of all backbone atoms (N, C α, C, O), were calculated using:

$$\Delta r = 1/N \sum_{i=1}^{N} \{[r_{i1} - r_{i2}]^2\}^{1/2}, \quad (1)$$

where r_{i1} and r_{i2} are the positions being compared and the summation is either for the individual atoms or over the backbone or sidechain atoms of the individual residues. RMS fluctuations, ΔR, were calculated using:

$$\Delta R = 1/N \sum_{i=1}^{N} \{\langle[(\Delta x_i)^2 + (\Delta y_i)^2 + (\Delta z_i)^2]\rangle\}^{1/2}, \quad (2)$$

where Δx_i, Δy_i and Δz_i are the differences between the reference and instantaneous atomic coordinates for the ith atom, $\langle\ \rangle$ represents the time average and the summation is either for the individual atoms or over the backbone or sidechain atoms of the individual residues. Interaction energies were calculated using the same potentials as used in the simulations.

Results

The potential energy of the two simulations, presented in Fig. 1 a and b, initially relaxes in a similiar fashion, however, in the VS the potential energy of the system drops a second time at approximately 100 ps. For both simulations the RMS difference between the backbone atoms and the X-ray structure as a function of time (Fig. 1 c) also underwent an initial fast relaxation followed by a stabilization, with a marked decrease in the rate of change, indicating that both simulations were

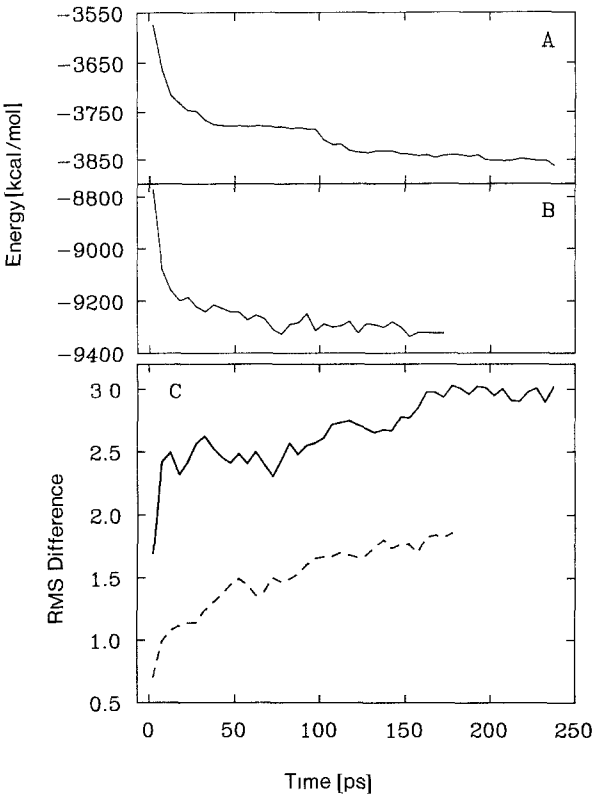

Fig. 1 A–C. Total potential energy of the **A** vacuum simulation and the **B** stochastic boundary simulation as a function of time. **C** RMS difference in Ångströms between 5 ps time-averaged backbone atom (N, C α, C, O) positions from the vacuum simulation (*line*) and stochastic boundary simulation (*dash*)

fairly well equilibrated. To avoid complications associated with the potential energy decrease in the VS the time-range of 120 to 240 ps was selected for analysis while the 53 to 176 ps time range was used from the SBS simulation.

To examine changes in the structures which occur during the two simulations the RMS differences between the backbone atoms from the X-ray structure and the SBS or VS time-averaged MD structures are presented in Fig. 2 a and b, respectively. Comparison of the differences for the two simulations show them to generally be smaller in the SBS in accordance with Fig. 1 c. Of the most significant changes in the VS are those in the region of residues 38 to 60, which encompasses many of the residues which define the enzyme's active site. On the other hand residues 20 to 26, which lie at the C-terminal of the α-helix, change much more in the SBS as compared to the VS.

To aid in the analysis the active site it will be separated into the recognition site, designated RS, and the catalytic site, designated CS (MacKerell et al. 1988). Residues in the RS include 42 to 46 and 98, all of which interact with the guanine base in the 2′GMP-RNase T1 X-ray structure (Arni et al. 1988). Comprising

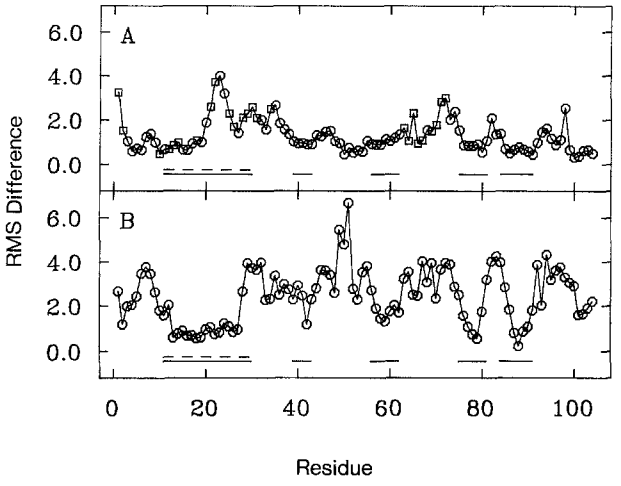

Fig. 2A and B. RMS difference by residue for the backbone atoms (N, C α, C, O) from the time-averaged simulation structures and the X-ray structure for the **A** stochastic boundary simulation and the **B** vacuum simulation. Units are in Angstroms. *Circles* represent residues subjected to the Verlet algorithm and *squares* to the Langevin algorithm. Residues in the α-helix are underscored with ——— and in the β-pleated sheets with ·····

Table 1. RMS Differences between the X-ray positions of active-site residues and the time-averaged MD positions in the 2′GMP-RNase T1 simulations

Residue	SBS		VS	
	Backbone	Sidechain	Backbone	Sidechain
RS region				
42	0.90	1.30	1.17	1.30
43	0.91	3.03	2.30	2.74
44	1.32	1.88	2.79	4.16
45	1.27	1.85	3.63	2.95
46	1.48	1.07	3.61	2.84
98	2.53	4.48	3.30	2.83
CS region				
40	0.95	1.33	2.92	2.97
58	0.91	1.55	1.45	3.08
77	0.86	1.65	1.08	3.00
92	0.98	1.69	3.87	3.75

Units are in Angstroms

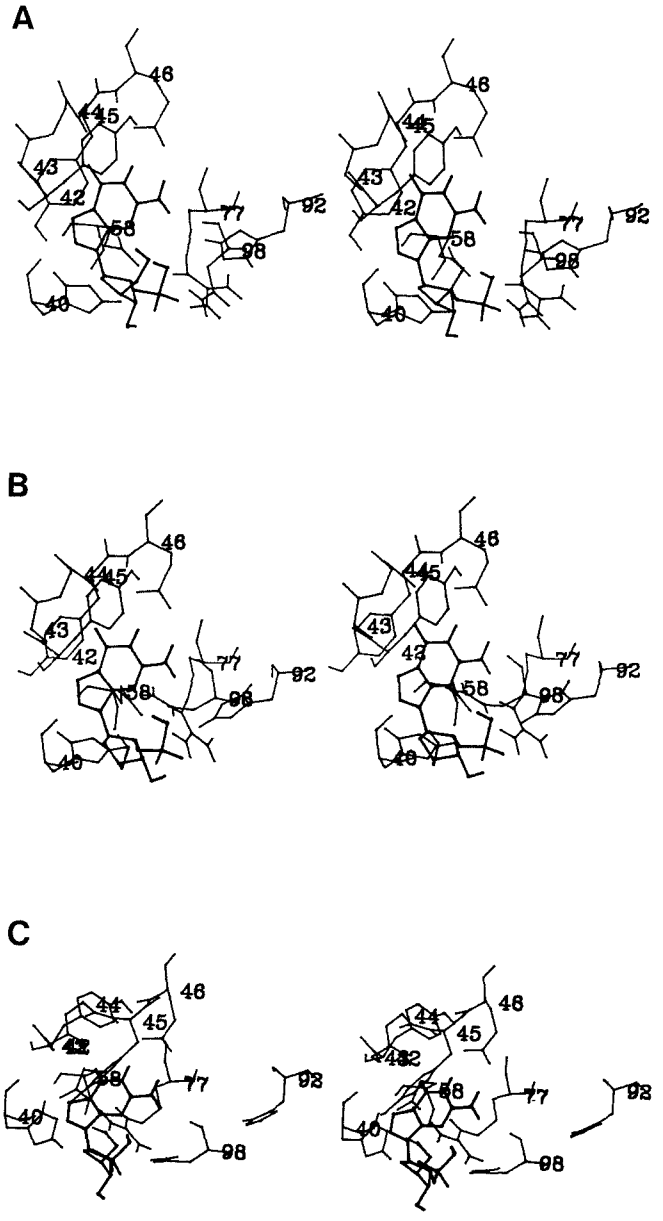

Fig. 3A–C. Stereodiagrams of the active-site structures from the **A** X-ray structure, the **B** time-averaged stochastic boundary simulation structure and the **C** time-averaged vacuum simulation structure. The sidechain atoms of *Asn*43 and *Asn*44 were ommitted. All protein backbone atoms were oriented to the same reference structure

the CS are residues 40, 58, 77 and 92 which interact with the phosphate moiety of 2′GMP and have been implicited to be involved in the catalytic mechanism (Takahashi and Moore 1982).

Figure 3 shows the active site from the X-ray structure (a) and the MD time-averaged active-site structures from the SBS (b) and the VS (c), respectively. Comparison of the two simulation active sites shows that the active site from the crystal structure is closer to the SBS than the VS active site. RMS differences between the active-site residue positions from the two simulations and the crystal structures are presented in Table 1. In general, the differences are smaller for the SBS, exceptions, however, exist with the sidechains of some of the RS residues. Further evidence of the maintenance of the active-site structure of the SBS is seen in Table 2 where the 2′GMP-protein hydrogen bonds are listed and in Table 3, showing the residue-residue hy-

Table 2. Hydrogen bonds between 2′GMP and Ribonuclease T1

Hydrogen bond				Distance [Å]		
Donor		Acceptor		X-ray	SBS	VS
RS region						
*Asn*43	H	2′GMP	N7	2.2	2.2	2.5
*Asn*43	H	2′GMP	O6	–	–	2.1
*Asn*44	H	2′GMP	O6	2.1	1.9	–
*Tyr*45	H	2′GMP	O6	2.1	2.5	–
2′GMP	H5T	*Tyr*45	OH	–	–	2.1
2′GMP	H1	*Glu*46	Oε1	2.0	2.0	2.0
2′GMP	H1	*Glu*46	Oε2	2.1	2.2	–
2′GMP	H21	*Glu*46	Oε2	2.0	2.0	2.0
*Asn*98	Hδ21	2′GMP	O2PT	2.2	–	–
*Asn*98	Hδ22	2′GMP	N3	–	2.2	–
2′GMP	H22	*Asn*98	O	2.0	–	2.3
2′GMP	H22	*Asn*98	Oδ1	–	2.3	–
CS region						
*His*40	Hε2	2′GMP	O1PT	2.0	2.0	2.0
2′GMP	H2T	*Glu*58	Oε1	2.5	2.5	–
2′GMP	H2T	*Glu*58	Oε2	2.1	2.2	–
*Arg*77	HH11	2′GMP	O2PT	–	–	1.9
*Arg*77	HH21	2′GMP	O1PT	–	2.4	1.9
*Arg*77	HH22	2′GMP	O1PT	2.4	2.2	–
*His*92	Hε2	2′GMP	O2PT	–	2.0	–

Hydrogen bonds between 2′GMP and active site residues following 120 steps of restrained ABNR minimization of the protein atom X-ray or time-averaged simulation coordinates. Criteria for hydrogen bond existence are hydrogen-acceptor distance ≤ 2.5 Å and donor-hydrogen-acceptor angle $< 65°$

Table 3. Hydrogen bonds between active-site residues in the X-ray and time-averaged simulation structures

Hydrogen bond				Distance [Å]		
Donor		Acceptor		X-ray	SBS	VS
RS region						
*Tyr*42	HH	*Glu*46	Oε1	2.0	2.1	2.0
*Asn*43	Hδ21	*Tyr*45	OH	–	–	2.2
*Tyr*45	H	*Glu*46	Oε1	–	2.3	2.5
CS region						
*His*40	O	*Glu*58	H	1.9	1.9	–
*Glu*58	H	*His*40	O	2.6	–	2.0
*His*40	Hδ1	*Glu*58	Oε1	–	–	2.0
*His*40	Hε2	*Glu*58	Oε2	2.5	2.2	–
*Arg*77	Hε	*Glu*58	Oε2	2.0	2.0	2.1
*Arg*77	HH22	*Glu*58	Oε2	–	2.0	1.8
RS–CS						
*His*92	Hε2	*Asn*98	O	2.2	–	–

Hydrogen bonds between 2′GMP and active site residues following 120 steps of ABNR minimization of the protein atom X-ray or time-averaged simulation coordinates. Criteria for hydrogen bond existence are hydrogen-acceptor distance ≤ 2.5 Å and donor-hydrogen-acceptor angle $< 65°$

Table 4. RMS Fluctuations of the active-site residues in the 2′GMP-RNase T1 simulations

Residue	SBS		VS	
	Backbone	Sidechain	Backbone	Sidechain
RS region				
42	0.56	0.67	0.53	0.68
43	0.67	0.91	0.60	0.85
44	0.74	0.87	0.77	1.08
45	0.86	1.27	0.78	1.23
46	1.03	0.84	0.95	0.68
98	0.75	0.90	0.59	0.95
CS region				
40	0.50	0.59	0.47	0.65
58	0.48	0.53	0.56	0.86
77	0.57	0.55	0.47	0.68
92	0.95	1.00	0.66	0.77

Units are in Angstroms

Table 5. RMS Fluctuations of non-hydrogen atoms in 2′GMP

Atom	Fluctuations [Å]	
	SBS	VS
Base		
N1	0.72	0.44
C2	0.69	0.44
N2	0.77	0.58
N3	0.66	0.49
C4	0.63	0.45
C5	0.66	0.44
C6	0.71	0.45
O6	0.81	0.60
N7	0.71	0.55
C8	0.72	0.58
N9	0.64	0.52
Sugar		
C1′	0.63	0.61
C2′	0.62	0.54
O2′	0.70	0.44
C3′	0.69	0.71
O3′	0.91	0.70
C4′	0.73	0.91
O4′	0.71	0.91
C5′	0.99	1.14
O5′	1.17	1.97
Phosphate		
PT	0.62	0.39
O1PT	0.60	0.44
O2PT	0.68	0.47
O2T	0.64	0.43

drogen bonds. Again, there is good agreement between the X-ray and the SBS structure in both the RS and CS regions of the active site.

Listed in Table 4 and Table 5 for both simulations are the RMS fluctuations for the active-site residues and for 2′GMP, respectively. The active-site fluctua-

Table 6. Interaction energies between 2'GMP and Ribonuclease T1 in the X-ray and the SBS and VS time-averaged structures

2'GMP region	Engergy [kcal/mole]		
	X-ray	SBS	VS
Base			
VDW	−20.3	−22.5	−21.9
Ele	−50.5	−42.1	−42.8
Total	−70.7	−64.6	−64.7
Sugar			
VDW	−4.3	−6.0	−6.0
Ele	−4.4	−11.6	−16.4
Total	−8.7	−17.6	−22.4
Phosphate			
VDW	−10.8	−9.9	−9.8
Ele	−95.2	−113.2	−139.7
Total	−106.0	−123.1	−149.5
2'GMP			
VDW	−35.3	−38.4	−37.3
Ele	−150.1	−166.9	−198.8
Total	−185.4	−205.3	−236.6

All structures were subjected to 120 steps of restrained ABNR minimization prior to calculations. VDW = van der Waals, Ele = electrostatic

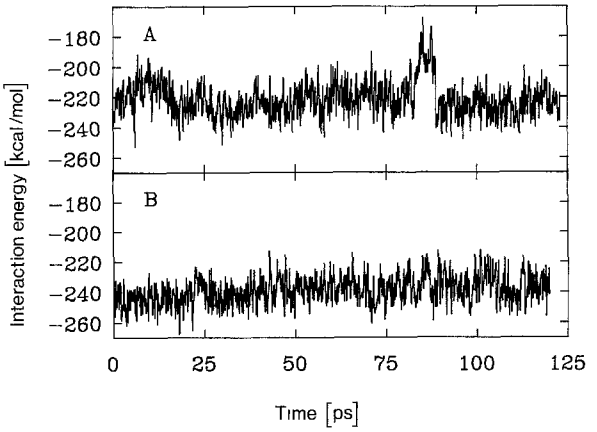

Fig. 4 A and B. Interaction energy between 2'GMP and RNase T1 versus time from the **A** stochastic boundary simulation and **B** the vacuum simulation

tions are similar for the two simulations. In the case of 2'GMP, however, there is an increased motion in the SBS. The only exceptions occur with atoms C4', O4', C5', and O5', where an increase in mobility occurs in the VS as compared to the SBS. RMS fluctuations for the entire enzyme will be presented elsewhere (MacKerell et al. submitted to J. Mol. Biol.) along with the temperature factors from the X-ray studies (Arni et al. 1988).

To further examine the interaction between the inhibitor and the enzyme the interaction energy, calculated using the same empirical energy function as in the simulations, between 2'GMP and all protein atoms was determined for the X-ray and the MD time-averaged simulation structures. Results, presented in Table 6, are separated into the guanine base, the sugar, the phosphate moiety and the total molecule. Overall, the values for all three structures are in agreement, although better agreement with the crystal structure occurs in the SBS. It should be emphasized that the interaction energies presented represent only the potential energy between the groups listed and are not related to any experimental thermodynamic parameters (Brown and Kollman 1987).

Analysis of the interaction energy as a function of time for both the SBS and the VS is presented in Fig. 4a and b, respectively. In the case of the VS the energy stays approximately constant throughout the simulation. In the SBS, however, at 82 ps (corresponding to 135 ps in Fig. 1) the interaction energy becomes less favorable by approximately 30 Kcal/mole. Further analysis of this phenomenon indicates that the interaction energy loss is related to changes around the phosphate moiety of 2'GMP (not shown). Next, examination of the interaction energies of the individual CS residues which interact with the 2'GMP phosphate moiety in the time region that the energy change occurs (Fig. 5) show *His*92 to be responsible for the less favorable interaction energy.

Discussion

The simulations are well equilibrated, as shown in Fig. 1, where after initial relaxation of the structures the changes in both potential energy and RMS differences with time were minimal in agreement with previous studies (van Gunsteren and Berendsen 1984; Krüger et al. 1985; Post et al. 1986; Åqvist et al. 1986). In the VS the drop in the potential energy at 100 ps is not distinctly seen in the RMS difference (Fig. 1), indicating that the change in the enzyme is not global in nature. Analysis of the VS time-averaged structures from 40 to 90 ps and 120 to 240 ps of the VS (not shown) reveals a shift in the position of the 2'GMP phosphate group and CS residues which interact with the phosphate. This shift encompasses a change of structure in the CS region from one similar to those occurring in the X-ray and SBS to that observed in the VS (Fig. 2). Problems, however, were avoided by selecting the time region of the VS after the shift for analysis, since it was related to a change in the equilibrium structure to a more favorable potential energy rather than a fluctuation of the equilibrium structure as occurs in the SBS simulation (see below).

Analysis of the overall structural changes in the two simulations (Fig. 2) shows the differences to be smaller in the SBS indicating the influence of water to

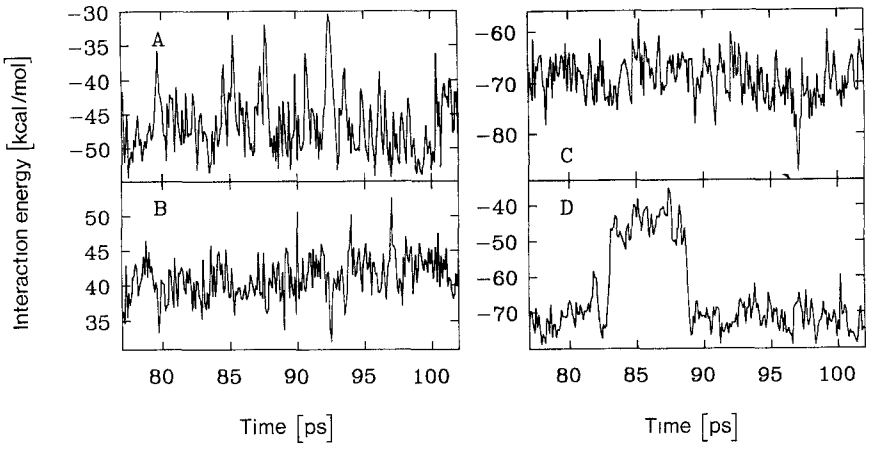

Fig. 5 A–D. Interaction energy between the 2′GMP phosphate moiety and the sidechain atoms of **A** *His*40, **B** *Glu*58, **C** *Arg*77 and **D** *His*92 versus time

maintain the enzyme structure in the simulation. Some of the SBS residues (20 to 26), however, exhibit larger differences than in the VS. Of these residues several were in the Langevin region of the SBS indicating that the differences may be an artifact. Significant differences, however, also occur in other Langevin residues (region 63 to 72) in which large differences also occur in the VS suggesting the importance of allowing residues outside of the waterball the freedom to move, which are partially restricted in the normal stochastic boundary approach (Brooks and Karplus 1983; Brünger et al. 1984; Brooks et al. 1985). Such restriction of movement at the boundary surface may influence phenomena occurring within the waterball and complicate the interpretation of results (McCammon and Harvey 1987).

Stereodiagrams of the three active-site structures, presented in Fig. 3, show that all three structures are similar; the guanine moiety interacts with the RS residues, sugar-protein interactions only occur with *Asn*98 in the simulation structures and the phosphate moiety interacts with CS residues. RMS differences in the RS region of the simulation structures (Table 1) reveal little change in the SBS, except in the case of *Asn*98, while larger changes generally occur in the VS. This is supported by the maintenance of hydrogen bonds in the SBS as compared to the X-ray structure (Table 2). Important hydrogen bonds which are maintained include those involving the backbone atoms of residues 43 to 45 with the N7 and O6 2′GMP atoms and of the *Glu*46 sidechain with the H1 and H21 atoms of 2′GMP. These interactions yield a well organized pattern which would be lost in the presence of other nucleic acid bases and thus, constitutes the mode of recognition in RNase T1 (Heinemann and Saenger 1982). In the case of the VS larger structural changes in the RS generally occur (Table 1) leading to a loss of several hydrogen bonds and the concomitant formation of new bonds (Table 2). Simultaneously, the rearrangement of the active site leads to the formation of several residue-residue interactions which are not observed in either the X-ray or SBS structures (Table 3). Overall, the changes in the VS result in a loss of several important 2′GMP-protein hydrogen bonds which do not occur in the SBS simulation, again indicating the importance of using water in the simulation to maintain the proper protein-inhibitor interactions.

As in the RS, the CS structure is similar in the X-ray and SBS structures while the VS structure differs from the other two (Fig. 3, Table 1). With the X-ray structure three of the four CS residues interact directly with the phosphate moiety (Table 2) while in the SBS structure all four CS residues are hydrogen bonded to the phosphate. Of note is the lack of a hydrogen bond with *His*92 in the X-ray structure which is present in the SBS structure which, by chemical modification, NMR (Takahashi and Moore 1982) and gene manipulation experiments (Nishikawa et al. 1987), has been indicated to be involved in the catalytic mechanism of RNase T1. Analysis of the $P2_12_12_1$ crystal contacts of ribonuclease T1 (Arni et al. 1987) reveals hydrogen bonding between the backbone atoms of *His*92, *Ala*95 and *Gly*97 with those of *Ala*1 and *Cys*2 across the two-fold screw axis along with a number of non-bonded contacts. Thus, the protein-protein intermolecular interactions in the RNase T1 crystals may influence the position of the *His*92 sidechain, suggesting that the solution *His*92 position may be similar to that observed in the SBS structure.

The above protein-protein crystal interactions may also influence the position of *Asn*98 leading to the relatively large positional shift in that residue between the X-ray and SBS structures (see Table 1). Furthermore, in the X-ray structure it is thought that *Glu*58 is protonated (neutral) allowing it to hydrogen bond to the O3P phosphate oxygen (Arni et al. 1988) while in the present study *Glu*58 is negatively charged, allowing the single protonated oxygen on the phosphate, OP2, (Saenger 1984) to hydrogen bond with *Glu*58 and possibly contributing to some difference

between the structures. With the VS simulation a number of the CS residue-phosphate moiety hydrogen bonds are lost, while an increase in hydrogen bonding occurs with *Arg*77 (Table 2). Some of the lost hydrogen bonds are replaced by several residue-residue hydrogen bonds (Table 3) all of which involve *Glu*58. Analysis of the active-site structures (Fig. 3) show that this residue moves back away from the phosphate moiety, which is related to the potential energy drop at 100 ps of the VS simulation.

RMS fluctuations of active-site residues are similar in both the RS and CS of the SBS and VS (Table 4) in contrast to results observed in free RNase T1 (MacKerell et al. 1988). An exception occurs with *His*92, which had an increased mobility in the SBS simulation. This higher mobility may be related to the change in the interaction energy of that residue with the phosphate moiety at 82 ps of the SBS (see below). With 2′GMP, however, there is generally a higher mobility in the SBS as compared to the VS except for the 4′ and 5′ atoms of the ribose moiety. The pattern of similar mobilitites for the active-site residues in the two simulations while the 2′GMP mobility increases in the SBS indicates the dominance of residue-residue interactions on the active-site residue fluctuations. This may possibly be due to the exclusion of water from those residues by 2′GMP, while with 2′GMP the influence of water, which is directly interacting with the inhibitor (MacKerell et al. submitted to J. Mol. Biol.), leads to an increase in mobility. For the 4′ and 5′ ribose atoms, which have an increased mobility in vacuum, there are no interactions with the protein (Table 2) indicating a possible damping effect of water on their motions in the SBS. Thus, it appears that in instances where protein-inhibitor non-bonded interactions occur the presence of water leads to an increase in flexibility, however, with the portion of the inhibitor not involved in non-bonded interactions and highly exposed to the solvent (or analogously a protein sidechain) the presence of water leads to a damping of the motion.

Analysis of the interactions energies (Table 6) between 2′GMP and the protein again reveals better agreement between the X-ray and SBS structures versus the VS structure. In all three cases the majority of interaction energy occurs in the region of the phosphate moiety followed by the guanine base, while with the sugar moiety very little interaction energy is present. Closer examination of the contribution of various RS residues towards the interaction energy with the guanine base is presented in Table 7. The largest contribution occurs with the sidechain of *Glu*46 which, via the Oϵ1 and Oϵ2 atoms, forms two hydrogen bonds with the base (Table 2). Other significant contributions occur with the backbone atoms of *Asn*43 and *Asn*44 which also form hydrogen bonds to the base. Of particular interest are the interactions of the *Tyr*42 and 45 sidechains with the base due to their formation of a sandwich structure with the base (Heinemann and Saenger 1982). With the present potential energy function the van der Waals contributions are somewhat favorable, albeit small, and with *Tyr*42 cancelled out by the electrostatic interactions. This low interaction energy supports the suggestion that the role of the tyrosines, which are conserved in the ribonucleases from various fungi (Hill et al. 1983), are to provide a hydrophopic environment for the base and thus help to exclude water molecules which could possibly compete for the guanine-protein hydrogen bonds rather than directly contributing to the interaction energy (MacKerell et al. submitted to J. Mol. Biol.).

To further investigate the interaction energy between 2′GMP and the protein the interaction energies for the two simulations are plotted as a function of time (Fig. 4). In the VS the interaction energy remains relatively constant throughout the simulation while in the SBS a marked change leading to a less favorable interaction energy occurs at 82 ps followed by a return to the initial range of values after approximately 5 ps. Closer examination of the interaction energies of the CS residue sidechains as a function of time (Fig. 5) shows that the change is solely related to the interac-

Table 7. Interaction energies between 2′GMP guanine moiety and recognition site residues in the X-ray and the SBS and VS time-averaged structures

Residue	Energy [kcal/mole]		
	X-ray	SBS	VS
*Tyr*42			
BKB	−3.5	−3.6	−3.5
SDC	−0.3	0.0	0.7
*Asn*43			
BKB	−6.8	−7.5	−7.5
SDC	−1.1	−0.5	−1.6
*Asn*44			
BKB	−3.5	−3.3	1.1
SDC	−0.3	−0.3	−0.2
*Tyr*45			
BKB	−0.7	0.4	2.9
SDC	−5.2	−2.7	−2.5
*Glu*46			
BKB	0.9	1.1	0.4
SDC	−41.4	−40.6	−41.7
*Asn*98			
BKB	−4.3	−0.5	−4.6
SDC	−1.7	−3.7	1.3

All strucutures were subjected to 120 steps of restrained ABNR minimization prior to calculations. BKB = backbone (N, Cα, C, O), SDC = sidechain (atoms including and beyond Cβ)

tion between the phosphate and *His*92. Presented in Fig. 6 are two time frames, one at 82.4 ps just prior to the change and a second at 83.4 ps during the period of less favorable interaction energy. As may be seen the decrease in energy is associated with the sidechain of *His*92 moving away from the phosphate leading to a loss of favorable electrostatic interactions between the negative phosphate group and the positive *His*92 sidechain including the breaking of the *His*92 H∈2 –2′GMP O2PT hydrogen bond (Table 2). The interaction energy then increases again when *His*92 moves back to its initial position (not shown). This motion can be described as an equilibrium fluctuation since it occurs when the enzyme is well equilibrated and then moves back, after a short period, to its initial position. Although it may be an artifact of the simulation, such transient fluctuations have previously been suggested by Cooper (1976) to be likely to occur. Furthermore, the nature of the fluctuation suggests an interesting situation where the enzyme, with the inhibitor bound, momentarily shifts to a configuration where the inhibitor is not so tightly bound. Such a configuration would offer an opportunity for the inhibitor to dissociate from the enzyme.

The stereodiagram in Fig. 7 of the superposition of the MD time-averaged 83.5–88.5 ps structure from the SBS and the time-averaged CS residues from a simulation of free RNase T1 including water (Mac Kerell et al. 1988) shows that during the period of lowered interaction energy *His*92 moves to a position similar to that observed in free RNase T1. Such a similarity in the *His*92 position between the two enzyme forms is reminiscent of the idea that a conformational change from one equilibrium conformer to another involves a shift in the probability that a specific conformer is being sampled in an equilibrium situation (Steitz et al. 1982). Thus, in the presence of 2′GMP the enzyme is primarily sampling a conformation like that presented in Fig. 6a, however, equilibrium fluctuations of the system occur such that low probability conformers are on occasion also sampled, as is seen during the period of less favorable interaction energy (Fig. 6b). The sampling of this low probability conformer, which results in a loss of favorable protein-inhibitor interaction energy, presents an opportunity for the inhibitor to dissociate from the enzyme and, thus, change the probability that specific conformers will be sampled. Thus, the fluctuation may lead to a conformational change in the enzyme leading to a conformer similar to that observed in the free enzyme (Fig. 7).

The presence of this equilibrium fluctuation makes it tempting to calculate some type of rate constant which may be associated with an experimentally determined rate. Considering that the off rate for 2′GMP

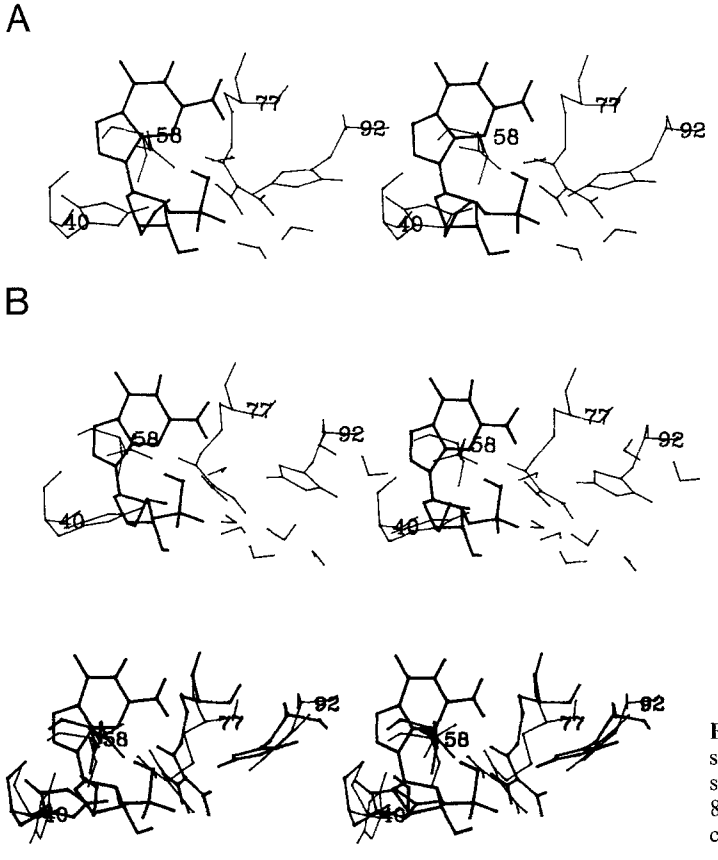

Fig. 6. Stereodiagrams of the catalytic-site structures from the stochastic boundary simulation at **A** 82.4 ps and **B** 83.4 ps. Times refer to Figs. 4 and 5. All protein backbone atoms were oriented to the same reference structure

Fig. 7. Superposition stereodiagrams of the catalytic-site structures from the MD time-averaged SBS free RNase T1 structure (*thin lines*) (MacKerell et al. 1988) and the 83.4–88.4 ps MD time-averaged SBS 2′GMP-RNase T1 complex structure (*thick lines*)

at 300 K is approximately 100 s^{-1} as deduced from temperature-jump experiments (MacKerell Jr., A. D. unpublished results) and assuming that such an equilibrium fluctution as described above occurs on the order of 10^9 s^{-1} (once in 123 ps in the present simulation) the enzyme would sample in the range of 10^7 such low energy configurations prior to dissociation. Thus, the 2′GMP-enzyme complex may sample a number of low interaction energy configurations before one such a 'dissociating' configuration is reached. The requirement for the sampling of such a number of configurations may be interpreted to indicate that more than one residue, including the inhibitor itself, is involved in achieving the 'dissociating' configuration.

Conclusion

Simulations of the active-site of RNase T1 in the presence and absence of water show that water is important in maintaining the proper 2′GMP-protein interactions, as seen in the X-ray structure. Water also alters the fluctuations of the system, especially concerning the bound inhibitor 2′GMP. However, the results also show that the basic interactions between 2′GMP and RNase T1 are fairly well maintained in the VS indicating that the use of vacuum simulations to study changes beyond the active-site region, which may require longer simulations, is reasonable. Analysis of the active-site structure from the SBS simulation, combined with various experimental evidence (Takahashi and Moore 1982; Nishikawa et al. 1987), indicate that in solution the sidechain of *His*92 may directly interact with the phosphate moiety of 2′GMP supporting the suggested catalytic role of that residue (Nishikawa et al. 1987). Results also support the notion that the guanine-protein hydrogen bonding pattern is responsible for the specificity of RNase T1 for guanylic acid residues (Arni et al. 1988). Lastly, an apparent equilibrium fluctuation in the active site around the inhibitor suggests a possible relationship between motions occurring in the picosecond time range and the dissociation of 2′GMP which occurs in the millisecond domain.

Acknowledgements. This work was supported in Stockholm by a NATO Postdoctoral Fellowship from the NSF to ADM and grants from the Knut and Alice Wallenberg Foundation, the Swedish Natural Science Research Council and the Lisa and Johan Grönberg Foundation and in Berlin by the Sonderforschungsbereich 9 and the Fonds der Chemischen Industrie. We are grateful to Thore Olausson and the Department of Medical Information Processing, Karolinska Institutet for assistance with and use of the NORD-500 computer.

References

Adelman SA (1980) Generalized Langevin theory for many-body problems in chemical dynamics: Reactions in liquids. J Chem Phys 73:3145–3154

Ahlström P, Teleman O, Jönsson B, Forsen S (1987) Molecular dynamics simulations of parvalbumin in aqueous solution. J Am Chem Soc 109:1541–1551

Åqvist J, Sandblom P, Jones TA, Newcomer ME, Gunsteren van WF, Tapia O (1986) Molecular dynamics simulations of the Holo and Apo forms of retinol binding protein. J Mol Biol 192:593–604

Arata Y, Kimura S, Matsuo H, Narita K (1979) Proton and phosphorus nuclear magnetic resonance studies of ribonuclease T1. Biochemistry 18:18–24

Arni R, Heinemann U, Maslowska M, Tokuoka R, Saenger W (1987) Restrained least-squares refinement of the crystal structure of the ribonuclease T1-2′-Guanylic acid complex at 1.9 Å resolution. Acta Crystallogr B43:548–554

Arni R, Heinemann U, Tokuoka R, Saenger W (1988) Three-dimensional structure of the ribonuclease *2′GMP complex at 1.9 Å resolution. J Biol Chem (in press)

Berkowitz M, McCammon JA (1982) Molecular dynamics with stochastic boundary conditions. Chem Phys Lett 80: 215–217

Blackburn P, Moore S (1982) Pancreatic Ribonuclease. In: Boyer PD (ed) The enzymes, vol 15, 3rd edn. Academic Press, New York, pp 317–433

Brooks B, Bruccoleri R, Olafson B, States D, Swaminathan S, Karplus K (1983) CHARMM: A program for macromolecular energy, minimization, and dynamics calculations. J Comp Chem 4:187–217

Brooks CL, Karplus M (1983) Deformable stochastic boundaries in molecular dynamics. J Chem Phys 79:6312–6323

Brooks CL, Brünger A, Karplus M (1985) Active site dynamics in protein molecules: a stochastic boundary molecular dynamics approach. Biopolymers 24:843–865

Brooks III C, Brünger A, Francl M, Haydock K, Allen LC, Karplus M (1986) Role of active site residues and solvation in RNase A. Ann NY Acad Sci 271:295–298

Brown FK, Kollman PA (1987) Molecular dynamics simulations of 'loop closing' in the enzyme triose phosphate isomerase. J Mol Biol 198:533–546

Brünger A, Brooks CL, Karplus M (1984) Stochastic boundary conditions for molecular dynamics simulations of ST2 water. Chem Phys Lett 105:495–500

Brünger AT, Brooks III CL, Karplus M (1985) Active site dynamics of ribonuclease. Proc Natl Acad Sci USA 82: 8458–8462

Cooper A (1976) Thermodynamics fluctuations in protein molecules. Proc Natl Acad Sci USA 73:2740–2741

Egami F, Oshima T, Uchida T (1980) Specific interaction of base-specific nucleases with nucleosides and nucleotides. Mol Biol Biochem Biophys 32:250–277

Frederick CA, Grable J, Melia M, Samduzi C, Jen-Jacobson L, Wang B-C, Greene P, Boyer HW, Rosenberg JM (1984) Kinked DNA in crystalline complex with EcoRI endonuclease. Nature 309:327–331

Gunsteren WF van, Karplus M (1982a) Protein dynamics in solution and in a crystalline environment: a molecular dynamics study. Biochemistry 21:2259–2274

Gunsteren WF van, Karplus M (1982b) Effect of constraints on the dynamics of macromolecules. Macromolecules 15: 1528–1544

Gunsteren WF van, Berendsen HJC (1984) Computer simulations as a tool for tracing the conformational differences between proteins in solution and in the crystalline state. J Mol Biol 176:559–564

Heinemann U, Saenger W (1982) Specific protein-nucleic acid recognition in ribonuclease T1-2′-Guanylic acid complex: an X-ray study. Nature 299:27–31

Hill C, Dodson G, Heinemann U, Saenger W, Mitsui Y, Nakamura K, Borisov S, Tischenko G, Polyakov K, Pavlovsky S

(1983) The structural and sequence homology of a family of microbial ribonucleases. Trends Biochem Sci 8:364–369

Jorgensen WL, Chandrasekhar J, Madura JD, Impey RW, Klein ML (1983) Comparison of simple functions for simulating liquid water. J Chem Phys 79:926–935

Karplus M, McCammon JA (1981) The internal dynamics of globular proteins. CRC Crit Rev Biochem 9:293–349

Krüger P, Strassburger W, Wollmer A, Gunsteren WF van (1985) A comparison of the structure and dynamics of avian pancreatic polypeptide hormone in solution and in the crystal. Eur Biophys J 13:77–88

MacKerell Jr AD, Rigler R, Hahn U, Saenger W (1987a) Ribonuclease T1: interaction with 2′GMP and 3′GMP as studied by time-resolved fluorescence spectroscopy. In: Ehrenberg A, Rigler R, Gräslund A, Nilsson L (eds) Structure and function of biomolecules. Springer, Berlin Heidelberg New York (Springer Series in Biophysics, vol 1, pp 260–264)

MacKerell Jr AD, Rigler R, Nilsson L, Hahn U, Saenger W (1987b) Protein dynamics: A time-resolved fluorescence, energetic and molecular dynamics study of ribonuclease T1. Biophys Chem 26:247–261

MacKerell Jr AD, Nilsson L, Rigler R, Saenger W (1988) Molecular dynamics simulations of ribonuclease T1: Analysis of the effect of solvent on the structure, fluctuations and active site of the free enzyme. Biochemistry 27:4547–4556

McCammon JA (1984) Protein dynamics. Rep Prog Phys 47: 1–46

McCammon JA, Harvey SC (1987) Dynamics of proteins and nucleic acids. Cambridge University Press, Cambridge

McClarin JA, Frederick CA, Wang B-C, Greene P, Boyes HW, Grable J, Rosenberg JM (1986) Structure of the DNA-EcoRI endonuclease recognition comples at 3 Å resolution. Science 234:1526–1541

Nishikawa S, Morioka H, Kim HJ, Fuchimura K, Tanaka T, Uesugi S, Hakoshima T, Tomita K-I, Ohtsuka E, Ikehara M (1987) Two histidine residues are essential for ribonuclease T_1 activity as is the case for ribonuclease A. Biochemistry 26:8620–8624

Post CB, Brooks BR, Karplus M, Dobson CM, Artymiuk PJ, Cheetham JC, Phillips DC (1986) Molecular dynamics simulations of native and substrate-bound lysozyme. J Mol Biol 190:455–479

Reiher III WE (1985) Theoretical studies of hydrogen bonding. Ph.D. Thesis, Harvard University, Cambridge, Mass., USA

Richards FM, Wyckhoff HW (1971) Bovine pancreatic ribonuclease. In: Boyer PD (ed) The enzymes, 3rd edn, vol 4. Academic Press, New York, pp 647–707

Rüterjans H, Pongs O (1971) On the mechanism of action of ribonuclease T1: Nuclear magnetic resonance study on the active site. Eur J Biochem 18:313–318

Ryckaert JP, Ciccotti G, Berendsen HJC (1977) Numerical integration of the cartesian equations of motion of a system with constraints: molecular dynamics of n-alkanes. J Comp Phys 23:327–341

Saenger W (1984) Principles of nucleic acid structure. Springer, Berlin Heidelberg New York

Steitz TA, Harrison R, Weber IT, Leahy M (1982) Ligand induced conformational changes in proteins in mobility and function in proteins and nucleic acids. (CIBA Foundation symposium 93). Pitman, London, pp 25–46

Sugio S, Amisaki T, Ohishi H, Tomita K-I, Heinemann U, Saenger W (1985a) pH-induced change in nucleotide binding geometry in the ribonuclease T1-2′-Guanylic acid Complex. FEBS Lett 181:129–181

Sugio S, Oka K-I, Ohishi H, Tomita K-I, Saenger W (1985b) Three-dimensional structure of the ribonuclease T1-3′guanylic acid complex at 2.6 Å resolution. FEBS Lett 183: 115–118

Swaminathan S, Ichiye T, Gunsteren WF van, Karplus M (1982) Time dependence of atomic fluctuations in proteins: analysis of local and collective motions in bovine pancreatic trypsin inhibitor. Biochemistry 21:5230–5241

Takahashi K, Moore S (1982) Ribonuclease T1. In: Boyer PD (ed) The enzymes, 3rd edn, vol 15. Academic Press, New York, pp 435–468

Uchida T, Egami F (1971) Microbial ribonucleases with special reference to RNases T_1, T_2, U_2. In: Boyer PD (ed) The enzymes, 3rd edn, vol 4. Academic Press, New York, pp 205–250

Warshel A (1979) Calculations of chemical processes in solutions. J Chem Phys 83:1640–1652

Warshel A (1984) Dynamics of enzymatic reactions. Proc Natl Acad Sci USA 81:444–448

Warshel A, Russel ST (1984) Calculations of electrostatic interactions in biological systems and in solutions. Q Rev Biophys 3:283–422